ISSN 2321-807X

Adsorption of U(VI) from aqueous solution by Triocthylamine (TOA) functionalized magnetite nanoparticles as a novel adsorbent

Nemat Mansouri, Kamal Saberyan*, Mohammad Noaparast

Department of Mineral Processing, College of Engineering, Tehran Science and Research Branch, Islamic Azad University, Tehran, Iran

Ne.mansouri@gmail.com

NFCRS, Nuclear Science and Technology Research Institute, P.O. Box: 11365-8486 , Tehran, Iran

*Email: Saberyan@aeoi.org.ir

Mineral Processing Engineering Department, School of Mining Engineering, University College of Engineering, University Of Tehran, Tehran, Iran.

ABSTRACT

Adsorption of U (VI) from aqueous solutions was investigated using magnetically assisted chemical separation (MACS) process. In the present study, Triocthylamine (TOA) functionalized magnetite nanoparticles (TOAFMNPs) were applied as a novel adsorbent for adsorption of U (VI) from aqueous solutions. The effects of initial pH, Triocthylamine to magnetite nanoparticles weight ratio, amount of adsorbent, stirring time and initial U(VI) concentration on U(VI) adsorption efficiency were investigated by batch experiments. The adsorption of U(VI) using this adsorbent was pH dependent, and the optimal pH was 5.5. In kinetics studies, the adsorption equilibrium can be reach within 20 min., and the experimental data were well fitted by the pseudo-second-order model. The highest value of U(VI) adsorption (93.8%) was achieved in optimum conditions. The Langmuir isotherm model correlates well with the U(VI) adsorption equilibrium data for the concentration range 10-80 mg/l. The maximum U(VI) adsorption capacity onto adsorbent was 27.5 mg/g at room temperature. Present study suggests that TOAFMNPs could be employed as a potential adsorbent for U(VI) adsorption, and also could provide a simple and fast separation method for removal of U(VI) ion from solutions

Indexing terms/Keywords

U (VI); MACS process; Magnetite Nanoparticles; TOA; Adsorption isotherm; Kinetics

Academic Discipline And Sub-Disciplines

Chemistry, Mining, mineral processing

SUBJECT CLASSIFICATION

E.g., Mathematics Subject Classification; Library of Congress Classification

TYPE (METHOD/APPROACH)

Provide examples of relevant research types, methods, and approaches for this field: E.g., Historical Inquiry; Quasi-Experimental; Literary Analysis; Survey/Interview

ISSN 2321-807X

INTRODUCTION

It is a common practice to leach uranium ores with sulfuric acid and to remove the uranium by conventional solvent extraction or ion exchange methods. However, the mentioned methods are complex processes that suffer from large secondary wastes, significant chemical additives, solvent losses, complex equipment, and bulky design [1,2]. So magnetically assisted chemical separation (MACS) processes can employ magnetite nanoparticles (MNPs) coated with a selective solvent extractant as adsorbent and are mixed with the metal ions solution. The metal ions are selectively extracted onto the adsorbent surface because of the chelating or exchange properties of the adsorbent. The adsorbent are removed by magnetic filtration or simply recovered with a magnet. The metal ions can be concentrated into a small volume by stripping the metal ions off the surface using an appropriate stripping agent.

In the last decade, comprehensive investigations and developments were observed in the field of magnetite nanoparticles. These materials often have unique physical, chemical, structural, and magnetic properties allowing for use in the field of novel applications including chemical and physical separation, environmental, remediation and mineral processing [3-9]. Magnetite nanoparticles have the advantages of large surface area, high number of surface active sites and high magnetic properties, which cause high adsorption efficiency [10]. Magnetic nanoparticles, particularly Fe_3O_4 nanoparticles are gaining increasing attentions due to its unique magnetite properties and feasibility of preparation. But magnetite nanoparticles easily aggregate because of anisotropic dipolar attraction. Usually a protection layer is required to ensure its chemical stability and improve their dispersibility [11].

Research at Argonne National Laboratory in USA has already demonstrated the effectiveness of the MACS process for the separation of transuranics [12-14]., Strontium [15], cesium [16], and cobalt and nickel [1] Shaibu et al. have used Cyanex 923- coated magnetic particles for uptake of Th (IV), U (VI), Am (III) and Eu (III) from simulated nuclear waste solutions. They showed that MACS process for uranium adsorption has more efficiency over traditional solvent extraction [2] Nunez et al. evaluated extractant coated magnetite carriers for efficiently separation of radionuclides such as americium and uranium from acidic solutions. The separation of the uranium from acid solutions using TOPO and D2EHPA are three orders of magnitude higher than in traditional solvent extraction techniques. The separation was maximum (K_d=50000 mg/l) at low-acid concentrations (0.01 M) with 0.1 *M* TOPO/0.5M D2EHPA coatings on magnetic nanoparticles at 25°C and decreased at high-acid concentrations (up to 8 M) [12,13].

S. Sadeghi et al. studied silica-coated magnetite nanoparticles modified with quercetin. These magnetite nanoparticles were assessed as a new solid phase sorbent for extraction of uranyl ions from aqueous solutions. The adsorption equilibrium of uranyl ions onto the sorbent was explained by Langmuir isotherm and maximum monolayer adsorption capacity was found 12.33 mg/g. The synthesized sorbent was applied to extraction of uranyl ions from different water samples [17]. They also have synthesized ferromagnetic nanoparticles with an imprinted polymer coating that is capable of adsorbing and extracting uranyl ions. The performance of the material was compared to that of particles coated with a non-imprinted polymer. The adsorbent containing the imprinted coating displays higher adsorption capacity and better selectivity to uranyl ions. The method was successfully applied to the determination of uranyl ions in water samples [18].

The adsorption features of synthetic magnetite nanoparticles have been investigated by R. Leal and M. Yamaura [19] for removal of uranyl ions from nitric solutions. Batch experiments were carried out to investigate the adsorption of UO_2^{2+} ions from nitric solution (in pH 4 and 5) onto magnetic nanoparticles. Equilibrium adsorption isotherm was evaluated using Freundlich and Langmuir models. The adsorption was between 40% and 80% under conditions studied.

Based on authors' literature review, little research efforts have been made at investigation of uranium removal or adsorption by magnetite nanoparticles. In the present study, (TOA) Functionalized magnetite nanoparticles, as a novel adsorbent, are being used for adsorption of U (VI). In bath experiments the absorption behavior of U (VI) at various pHs was studied. To achieve maximum adsorption efficiency, various parameters affecting the U (VI) adsorption were studied and optimized.

1. Experimental

1.1. Materials

All chemicals including $FeCl_2.4H_2O$, $FeCl_3.6H_2O$, NaOH, HCl and Triocthylamine (Specific gravity: 0.891 g/ml) with analytical grade were supplied from Merck Company and were used without further purification. A stock solution of uranyl ions (100 mg/l U(VI)) was prepared by dissolving accurate quantity of $UO_2(NO_3)_2.6H_2O$ in deionized water. Other concentrations prepared from stock solution by dilution varied between 10-80 mg/l. Fresh dilutions were used for each experiment. The initial pH of the working solution was adjusted by the addition of dilute HCl or NaOH solutions.

1.2. Apparatus

U(VI) concentration in aqueous solution was determined by inductively coupled plasma optical emission spectrometry (ICP-OES) (Perkin-Elmer 2000 DV model). Synthesized nanoparticles were studied by X-ray powder diffraction (XRD) measurements (STADI-MP, STOE Company, with monochromatized Cu Kα radiation). FT-IR method (Bruker Vector 22 model) was used for functional groups investigations in the range of 4000-400 cm^{-1}. Synthesized nanoparticles were dispersed by ultrasonic cleaner (model clean 01). The pH of solution was measured using pH meter (model 827 Metrohm).

ISSN 2321-807X

1.3. Synthesis of magnetite nanoparticles (MNPs)

MNPs were prepared by normal co-precipitation method.[20-23] with iron salts ($FeCl_2.4H_2O$, $FeCl_3.6H_2O$) and polyethylene glycol (PEG) according to reaction (1). PEG ensures the suspension stability of MNPs. Briefly, 25 ml of $FeCl_2.4H_2O$ and $FeCl_3.6H_2O$ solutions was prepared in 0.6 M HCl and deoxygenized by argon inert gas for 15 minutes. 25 ml of 2 M NaOH was slowly dropped into a three neck flask containing iron chloride solutions under argon gas injection until pH=11.5, after which it was washed several times by distilled water until pH about 7. Finally, it was dried at 50° C for 24 hours, ground, and then characterized by XRD analysis

$$\mathbf{Fe^{2+} + 2Fe^{3+} + 8OH^- + PEG \rightarrow Fe_3O_4 + 4H_2O + PEG} \quad (1)$$

1.4. Preparation of the adsorbent (TOAFMNPs)

300 mg of magnetite nanoparticles were dispersed in diethyl ether by an ultrasonic bath for 1 hour. After removing from the bath, the appropriate amount of TOA (for example 0.04 ml TOA for TOA/MNPs (w/w) 10%) in diethyl ether was then added to it and left until diethyl ether evaporated and afterwards the stock of TOA-functionalized MNPs with concentration 3 g/l were prepared by addition of 100 ml deionized water. The adsorbent nanoparticles in aqueous solution were black emulsion with stability even after one month. They were easily separated from solution in a few seconds, under an external magnetic field. Observations demonstrated easy and fast separation of the adsorbent after the adsorption experiments.

1.5. Batch Experiments

All batch experiments were carried out in a beaker by mechanical stirrer at 300 rpm. The effect of variable parameters on adsorption were determined by equilibrating the adsorption mixture (50 ml) containing accurate amount of adsorbent and uranyl ions in different conditions. Under continuous mechanical stirring of the mixture for 20 min, the adsorption of uranyl ions from aqueous solution onto the adsorbent was allowed to proceed at room temperature. After standing for 1 min, the TOAFMNPs adsorbed uranyl ions were completely gathered to one side of the solution under a external magnetic and the clear supernatant was directly decanted. The amount of adsorbed U(VI) was determined from the difference between the U(VI) concentration in the aqueous before and after the adsorption. The percent adsorption (%) of U (VI) from solution was calculated as follows.

$$\text{Adsorption } (\%) = \frac{C_0 - C_e}{C_0} 100 \quad (2)$$

C_0 and C_e are concentration of U(VI) at initial and equilibrium time (mg/l), respectively. The adsorption capacity (q_e,mg/g) of uranium was achieved by the following equation.

$$q_e = \frac{(C_0 - C_e)V}{m} \quad (3)$$

V is the volume of the solution (ml), *m* the mass of adsorbent (g).

1.6. TEM and XRD study

In order to fully characterize the synthesized magnetite nanoparticles and adsorbent for morphology and structure, different techniques such as TEM, XRD, FT-IR were used. Fig. 1 shows the typical TEM images of the magnetite nanoparticles and TOAFMNPs. Most of the produced MNPs have sizes approximately less than 15 nm which are shown in Fig. 1a. Fig. 1b illustrates that the size of TOAFMNPs is 20–25 nm.

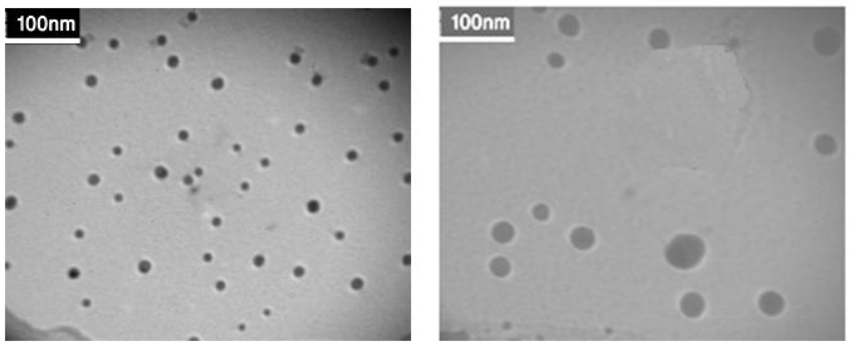

Figure 1. TEM images of nanoparticles. (a: magnetic nanoparticles (MNPs). b, TOA functionalized magnetite nanoparticles (TOAFMNPs))

To specify the structure of magnetite nanoparticles, X-ray diffraction patterns (XRD) were employed. According to Fig. 2, the powder XRD pattern of the synthesized magnetite nanoparticles was close to the pattern for crystalline magnetite Fe_3O_4. Using the most intense peak in magnetite nanoparticles XRD diffraction pattern, the particles size of approximately 10 nm was estimated by the Debye–Scherer formula [24], which was consistent with the results obtained from the TEM image**.** The characteristic peaks of pure Fe_3O_4 nanoparticles at 2θ = 30.1°, 35.4°, 43.9°, 54.4°, 57.0° and 63.6°, marked by their indices ((2 2 0), (3 1 1), (4 0 0), (4 2 2), (5 1 1), and (4 4 0)), which accorded well with the database (JCPDS 01-1111)

ISSN 2321-807X

were observed for synthesis of magnetite nanoparticles confirming the presence of the crystalline structure of the magnetite.

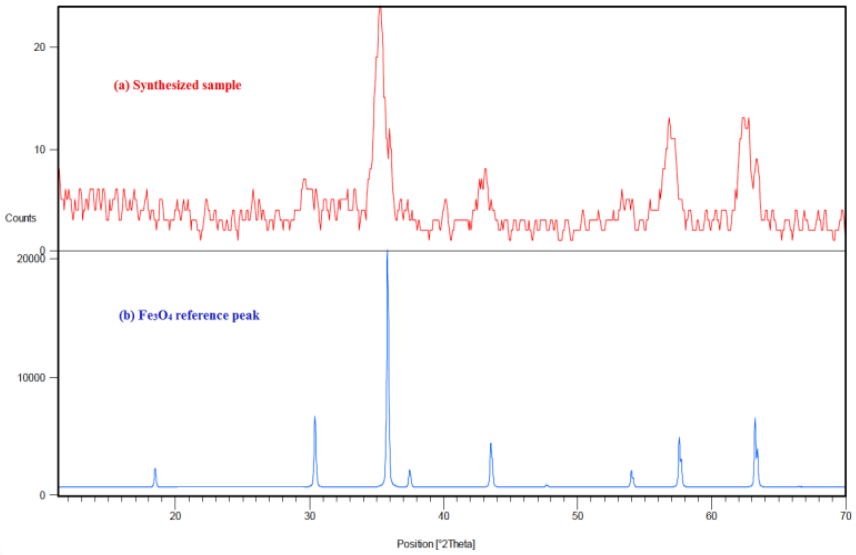

Figure 2. XRD pattern of (a) synthesized nanoparticles and (b) reference magnetite particles.

1.7. FT-IR spectrum of the adsorbent

TOA-functionalized magnetite nanoparticles were identified using Fourier transform infrared (FT-IR) spectrometry. The resulting spectra are shown in Fig 3. The functional groups of amine-functionalized magnetite nanoparticles were identified using FT-IR . The bands centered around 3451 cm^{-1} and 1634 cm^{-1} are, respectively, assigned to the O–H stretching and deforming vibrations of adsorbed water on the surface of nanoparticles. The strong IR band at 575 cm^{-1} is characteristic of the Fe–O vibration of Fe_3O_4. A band in the region of 2919 cm^{-1} was ascribed to asymmetric stretching of the C–H_2 groups. Two weak bands around 2919 cm^{-1} were attributed to symmetric stretching of C–H_2 and asymmetric stretching of C–H_3. A band at 1085 cm^{-1} assigned to C–N stretching vibrations. The results indicated that amino-group has been attached onto the Fe_3O_4 nanoparticles. Figure 4 shows the structural formula of TOA.

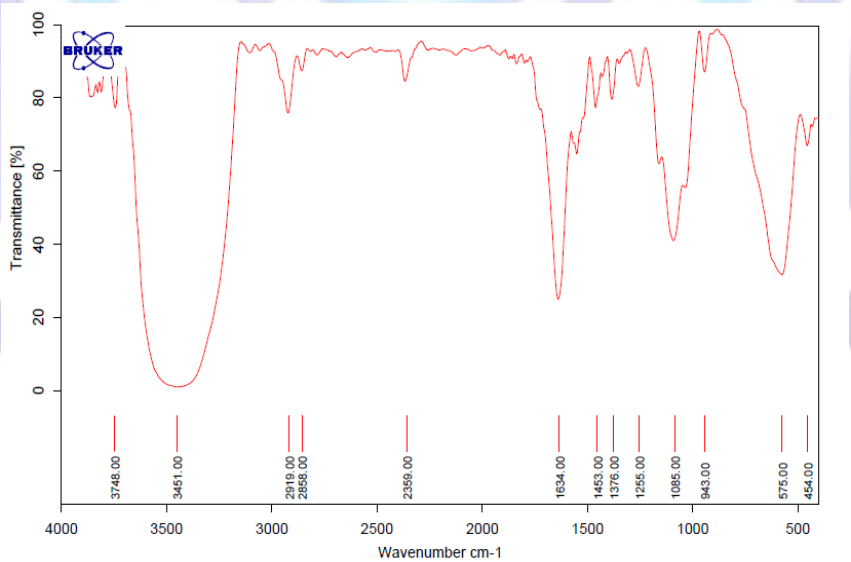

Figure 3. FT-IR spectrum of (a) Fe_3O_4 nanoparticles, (b) TOAFMNPs.

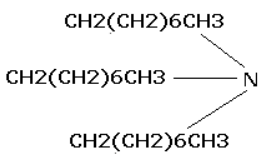

Figure 4. structural formula of TOA

ISSN 2321-807X

2. Results and Discussion

2.1. Effect of TOA/MNPs weight ratio (w/w)

Adsorption of U(VI) on TOAMNPs was studied by varying the TOA/MNPs weight ratio between 10 to 100% while keeping the other parameters constant. The adsorption as function of TOA/MNPs weight ratio is shown in Fig.5. According to this figure, adsorption of U(VI) at TOA/MNPs>10% is observed to be less since MNPs are stacked to each other and are inhibited dispersion in the solution during adsorption and decreased adsorption values. The maximum adsorption 58.2 % was achieved at 10% TOA/MNPs weight ratio.

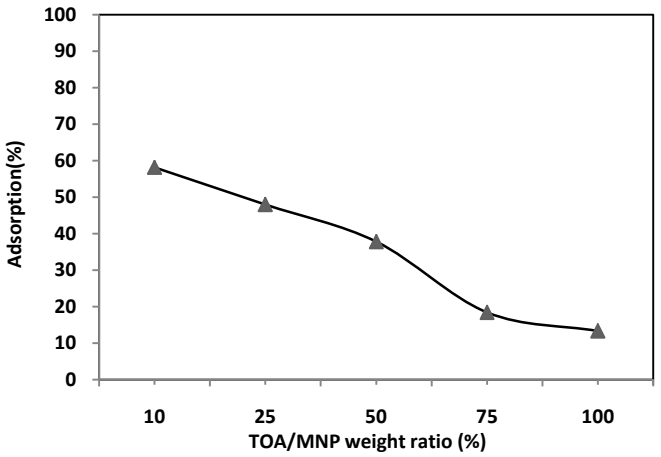

Figure 5. Effect of TOA/MNPs weight ratio on adsorption(%).

U (VI) concentration: 10 mg/l, adsorbent amount: 15 mg, stirring time: 20 min., pH=5.0

2.2. Effect of adsorbent amount

To optimize the adsorbent amount for 10 mg/l U (VI) adsorption, the adsorbent effect was studied in the range of 15 to 45 mg in 5 to 15 ml from stock of adsorbent with concentration 3g/l. The results of the experiments are showed in Fig.6. This results clearly demonstrated that the percentage adsorption increased from 60.2 to 94.8% with the increase of the TOAFMNPs amount and remains almost constant at about 30 mg with more than 91.8% adsorption. This increase in adsorption would be attributed to the availability of larger surface area and more adsorption sites. With increasing TOAFMNPs amount, the available sites on magnetite nanoparticles surfaces increase and provide more adsorption sites to adsorb metal ions, and thereby results in increasing of U(VI) adsorption. From the economical viewpoint and for guaranteeing quantitative adsorption of U (VI), the 30 mg adsorbent with 91.8% adsorption was selected as the optimum amount for further experiments.

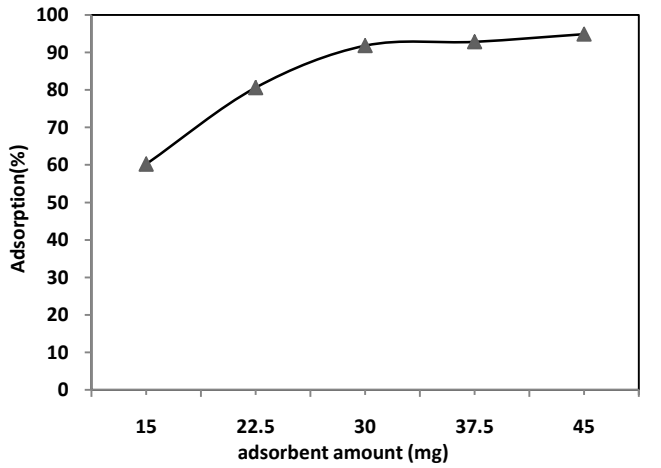

Figure 6. Effect of amount of adsorbent on adsorption(%), U (VI) concentration: 10 mg/l, TOA/MNPs: 10%, stirring time : 20 min., pH 5.00

ISSN 2321-807X

2.3. Effect of pH

According to Fig. 7 the pH value of the solution plays an important role in the whole adsorption process and particularly on the adsorption capacity. It is clear from the results that adsorption values increased along with increasing pH values. This result shows that the adsorption ability of adsorbent for U (VI) is high in near neutral conditions and low in strong acidic conditions. The maximum adsorption value for U (VI) onto TOAFMNPs was about 93.8. Therefore, it was found that the adsorption efficiency of U (VI) is high in pH 5.5 and it was selected for further adsorption experiments**.**

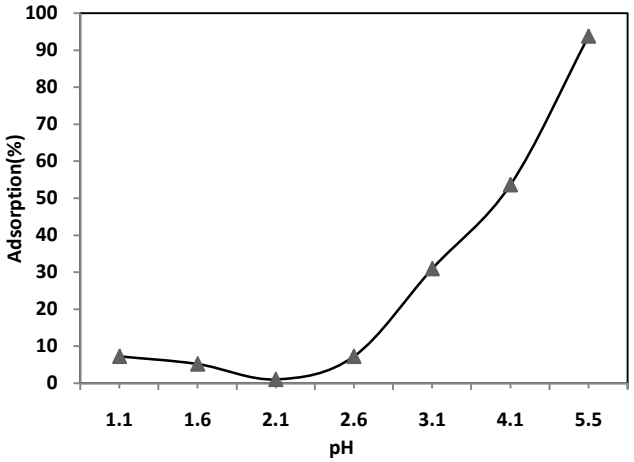

Figure.7. Effect of pH on adsorption of U (VI). U (VI) concentration:10 mg/l, amount of adsorbent: 30 mg, TOA/MNPs: 10%, stirring time : 20 min

It is well known that the species of uranium are strongly dependent on pH value. At lower pH values, the predominant species is UO_2^{2+}. When the pH increases, the uranium speciation in solution changes and the hydrolysis products such as $UO_2(OH)^+$, $[(UO_2)_2(OH)_2]^{2+}$ and $[(UO_2)_3(OH)_5]^+$ are formed (Fig.8).[26]

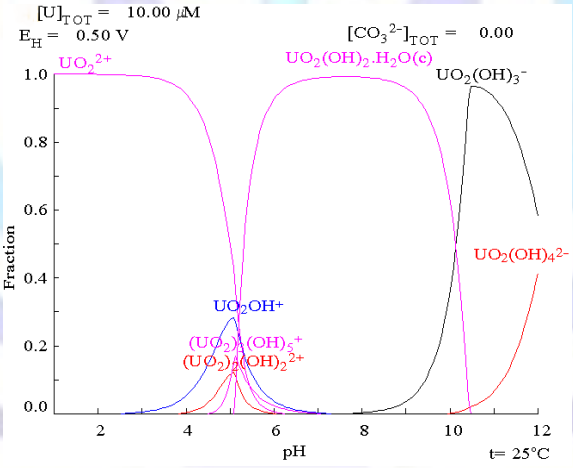

Figure .8. Fraction amounts of species uranium at different pH [23]

It can be induced that these species that are exchanged at the functional groups on the TOAFMNPs. It is well known that surface of the TOAFMNPs negatively charged hence it can absorb positively charged uranyl ion species or other hydrolyzed species through electrostatic interaction. At low pH, the H^+ ions present at acidic solution will also competes with positively charged uranium species for the adsorption sites resulting in reduced uptake of U(VI).

2.4. Effect of stirring time

The adsorption kinetics governing the residence time adsorption reaction determines the solute uptake rate or efficiency of adsorption. Hence, adsorption of U (VI) on TOAFMNPs was considered as a function of stirring time in the range of 5–50 min. Fig. 9 shows the time profile of U (VI) adsorption on TOAFMNPs in terms of percentage of adsorption and adsorption capacity

It was illustrated that adsorption U (VI) was rapid in first 10 min and then gradually attained equilibrium within 20 min (92.3% adsorption). The rapid adsorption rate has significant practical importance, which ensures high efficiency and cost-effectiveness. From the stiring time study, it is shown that 20 min of is enough to achieved equilibrium and hence subsequent adsorption experiments were conducted with 20 min stiring time.

ISSN 2321-807X

2.4.1 Adsorption kinetics

The kinetics of adsorption has to be studied to investigate the mechanism of adsorption. Four kinetic models were tested to fit experimental data of uranium adsorption on TOAFMNPs: pseudo-first-order, pseudo-second-order,

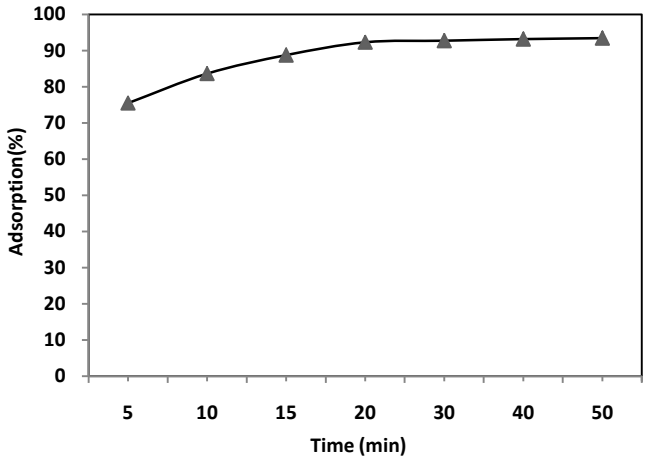

Figure.9: Effect of adsorption time on adsorption U (VI) concentration:10 mg/l, amount of adsorbent: 30 mg, TOA/MNPs: 10%, pH 5.5.

Elovich and Intra-particle diffusion model. Linear mathematical expressions of these models are given in Eqs. (4) – (7) respectively.

$$\log(q_e - q_t) = \log\left(-\frac{k_1 t}{2.303}\right) \quad (4)$$

$$\frac{t}{q_t} = \frac{1}{k_2 q_e^2} + \frac{1}{q_e} t \quad (5)$$

$$q_t = \frac{1}{\beta}\log(\alpha\beta) + \frac{1}{\beta}\log t \quad (6)$$

$$q_t = k_{id} t^{0.5} + C \quad (7)$$

Where q_e is the adsorption capacity at equilibrium (mg g^{-1}), q_t is the adsorption capacity at time t (mg g^{-1}), k_1 is the rate constant of the pseudo-first-order adsorption (min^{-1}), and k_2 is the rate constant of the pseudo-second- order kinetics (g mg^{-1} min^{-1}), α is the Elovich adsorption rate constant (mg g^{-1} min^{-1}), β is the Elovich desorption rate constant(g mg^{-1}) and *kid* is the intra-particle diffusion rate constant (mg g^{-1} $min^{-0.5}$). Pseudo-first and pseudo-second-order models are macro scopic kinetic models usually applied for describing adsorption process. This suggest that adsorption can be investigated as either first or second order chemical reaction where the adsorption process is the rate determining step. The possibility of intra-particle diffusion resistance affecting adsorption was explored using the appropriate intra-particle diffusion model.

In order to investigate the adsorption kinetics of U(VI) onto TOAFMNPs, the above four model were applied. The results of the experimental data fitting with these models for the adsorption of U(VI) onto TOAFMNPs are shown in Fig. 10 and the values are listed in Table 1. The closeness of calculated value of adsorption capacity (15.7 mg g^{-1}) at equilibrium time (q_e) from pseudo-second-order model to the experimental value (16 mg g^{-1}) ensures the applicability of pseudo-second-order kinetic model for the adsorption process. Also, the strongest correlation (R^2=0.999) support the description of pseudo-second order kinetic model. Therefore, chemisorptions may be the rate determining step of the adsorption process rather than mass transfer in solution.

ISSN 2321-807X

Table 1: Kinetic parameters for U(VI) adsorption on TOAFMNPs		
Kinetic Models	**Parameter**	**Value**
Pseudo-first-order	K_1 (min^{-1})	0.03
	q_e^{calc} (mg g^{-1})	2.85
	q_e^{exp} (mg g^{-1})	16
	R^2_1	0.754
Pseudo-second-order	K_2 (g mg^{-1} min^{-1})	0.05
	q_e^{calc} (mg g^{-1})	15.7
	q_e^{exp} (mg g^{-1})	16
	R^2_2	0.999
Intra-particle diffusion	h (mg g^{-1} min)	0.079
	K_i (mg g^{-1} $min^{0.5}$)	0.553
	C (mg g^{-1})	11.88
	R^2	0.761
Elovich	α (mg g^{-1} min^{-1})	13250
	β (g mg^{-1})	0.341
	R^2	0.884

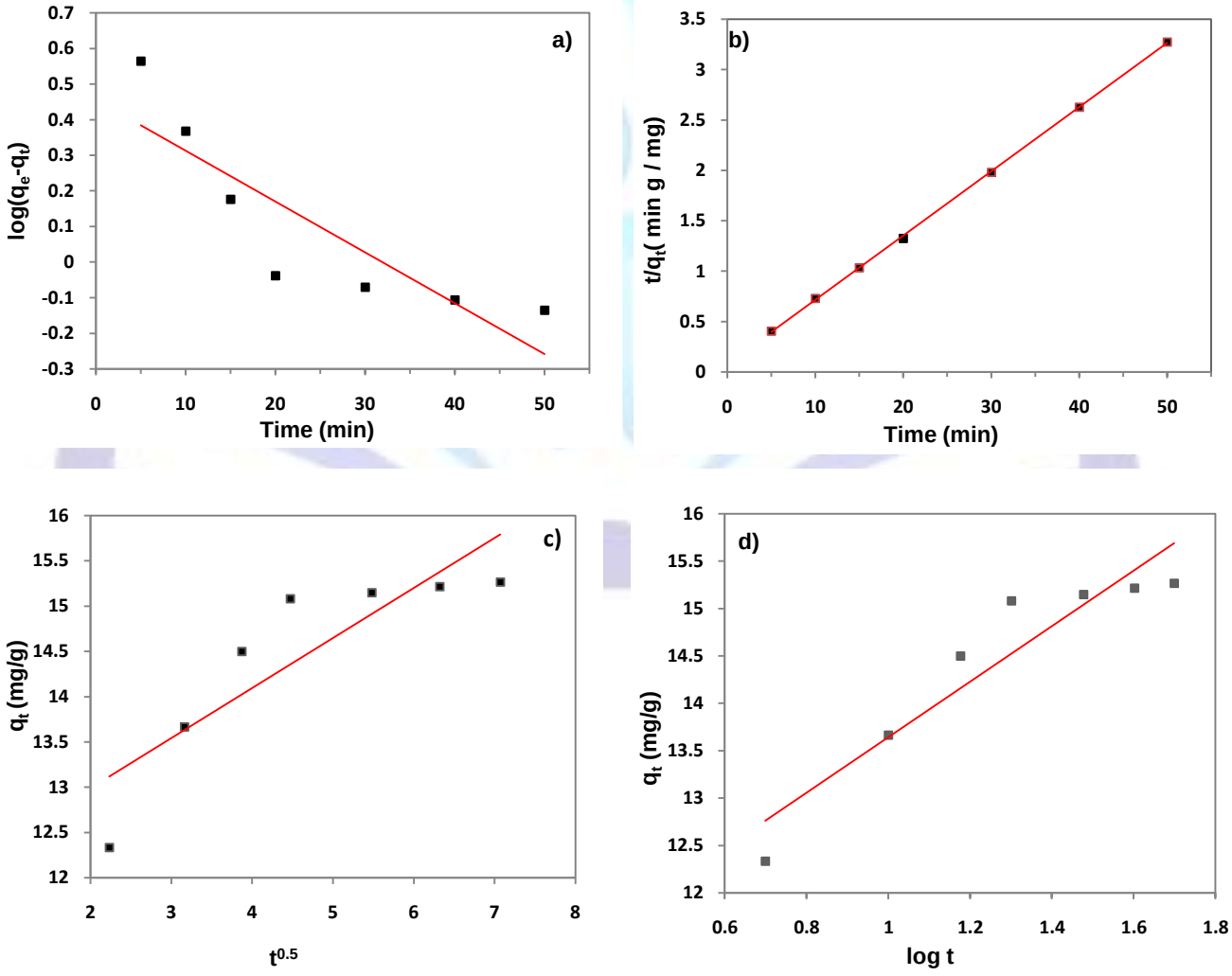

Figure. 10. kinetic adsorption study for U(VI) adsorption on TOAFMNPs according to (a) Pseudo-first-order, (b) Pseudo-second-order, (c) Elovich and (d) intra-particle kinetics models

ISSN 2321-807X

2.5. Effect of initial U(VI) concentrations

The relation between amount adsorbed and equilibrium concentration of U (VI) in aqueous solution is very important to describe the adsorption process. Fig. 11 depicts the adsorption capacity as a function of initial U(VI) concentration. It was observed that the amount of U (VI) adsorbed on the TOAFMNPs increases with increase in initial U (VI) concentration. This can be due to the increase in specific adsorption sites at the adsorbent surface which enhances the interaction between adsorbate and the adsorbent. This figure also shows that adsorption capacity was increased with increasing U (VI) concentration up to 33 mg l^{-1} and more increase in U (VI) concentration has no significant effect on adsorption capacity. This can be attributed to the saturation of specific adsorption sites on TOAFMNPs. The maximum adsorption capacity for U (VI) on was determined experimentally to be 27.5 mg g^{-1}.

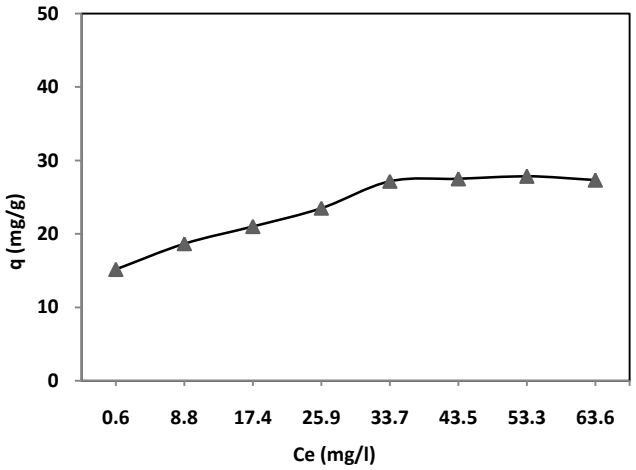

Figure. 11. Effect of initial U(VI) Concentration on adsorption capacity: Amount of adsorbent: 30 mg, TOA/MNPs: 10%, pH 5.5, stirring time : 20 min.

Table 2 provides the comparison of adsorption capacity of TOAMFNPs and other adsorbents for U (VI) adsorption. It can be seen that the adsorption ability of TOAFMNPs was about six times higher than that of magnetite nanoparticles. Hence, TOAFMNPs may be introduced as a good adsorbent for U (VI) ions with promising potential applications for the adsorption of U (VI) ions from aqueous solution due to specific separation method.

Table 2: kinetic parameters of U(VI) ions adsorption onto TOAFMNPS

Adsorbent	pH	Adsorption Capacity (mg/g)	Reference
TOA functionalized magnetite nanoparticles	5.5	27.5	This work
Silica-coated magnetite nanoparticles modified with quercetin	4-5	12.33	S. Sadeghi et al. (2012) [17]
Magnetite nanoparticles	7	5	Das et al. (2010) [26]
Modified clays with titanium oxide	3.5	0.582	Humelnicu et al. (2009) [27]
Magnetic oxide coated zeolite	4	15.1	Han et al. (2007) [28]
qoethite	6	33.96	Yusan and Erenturk. (2011) [29]
Natural sepiolite	3	34.61	Donat (2009) [30]

2.5.1. Adsorption isotherm

The equilibrium adsorption isotherm is of importance in the design of adsorption systems. Several adsorption isotherm equations are available and two important isotherms are selected in this study, the Langmuir and Freundlich isotherms. The equilibrium data obtained in the present study were analyzed using the linear forms of the expressions of Langmuir (Eq. (8)) and Freundlich (Eq. (9)) isotherm models:

$$\frac{C_e}{q_e} = \frac{1}{Q_0 b} + \frac{C_e}{Q_0} \quad (8)$$

$$logq_e = logK_f + \frac{1}{n} logC_e \quad (9)$$

where *Ce* is the equilibrium concentration (mg/l), q_e adsorption capacity at equilibrium (mg/g), Q_0 is the maximum amount

of adsorbate per unit weight of adsorbent to form a complete monolayer on the surface (mg/g); b is the Langmuir isotherm constant (l/mg), related to the affinity of the adsorption sites; KF [(mg/g) (l/mg)$^{1/n}$] and n are the Freundlich constants related to adsorption capacity and adsorption intensity of adsorbents, respectively.

Linear form of both model are graphically represented in Fig.12. The isotherm parameters of each model were calculated by linear regression analysis and the values are given in Table 3. From the value of R^2, it is concluded that the Langmuir isotherm fits the experimental data better than Freundlich model.

The results have also shown that the calculated adsorption capacity (Q_0 , 29.41 mg g^{-1}) from Langmuir isotherm model exhibits good agreement with the experimental value (27.5 mg g−1). Applicability of Langmuir model describes the monolayer adsorption of U(VI) on the surface of TOAFMNPs.

Table 3: Comparison of equilibrium isotherm models

Langmuir	
Q_0 (mg g^{-1})	29.41
b (L mg^{-1})	0.256
R^2	0.990
Freundlich	
K_f [(mg g-1)(L mg^{-1})1/n]	15.70
n	7.52
R^2	0.881

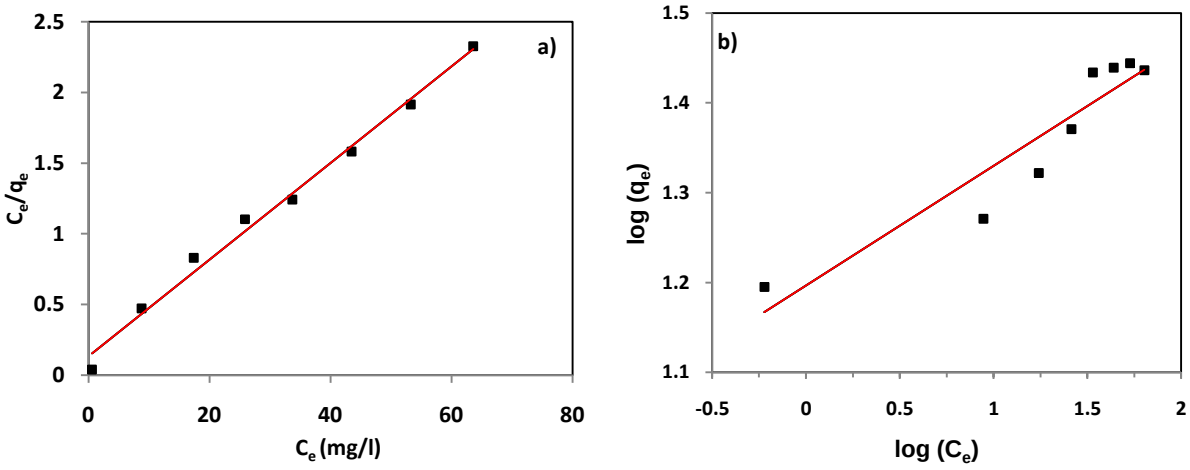

Figure. 12. (a) Langmuir, (b) Freundlich adsorption isotherm simulation of U(VI) adsorption on TOAFMNPs

A further analysis of the Langmuir equation can be made on the basis of a dimensionless parameter, R_L also known as separation factor and is given by following Eq. (10).

$$\boldsymbol{R_L = \frac{1}{1+bC_0}} \qquad (10)$$

R_L is defined by the ratio of unused adsorbent capacity to the maximum adsorbent capacity. The value of R_L indicates the nature of isotherm like unfavorable ($R_L > 1$), linear ($R_L = 1$), favorable ($0 < R_L < 1$) or irreversible ($R_L = 0$). It was observed that the calculated R_L values are between 0 and 1 for all tested uranium concentrations indicating that adsorption of U (VI) on TOPAFMNPs is favorable (Fig. 13).

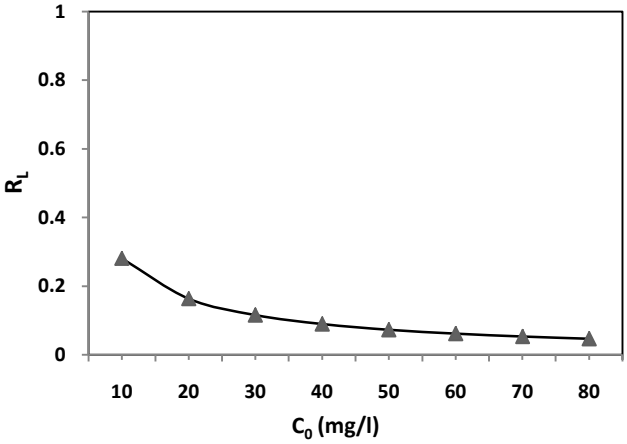

Figure. 13. R_L Values For all tested uranium Concentrations

3. Conclusion

A new adsorbent based on magnetite nanoparticles was synthesized and functionalized with TOA. The potential application of the functionalized magnetite nanoparticles as an adsorbent in the adsorption of U(VI) from aqueous solutions was investigated. The optimum conditions was achieved in initial pH 5.5, Triocthylamine to magnetite nanoparticles weight ratio 10% (w/w) , amount of adsorbent 30 mg, stirring time 20 min. and initial U (VI) concentration 10 mg/l. The adsorption ability of U (VI) on TOAFMNPs was strongly dependent on pH values. The adsorption isotherm of U (VI) can be described well by Longmuir model. Comparison of adsorption capacity of TOAMFNPs and other adsorbents for U (VI) shows that this new adsorbent with adsorption capacity was about 27.5 mg/g could be a perfect, fast and efficient candidate as adsorbent to adsorption U (VI) from aqueous solutions.

REFERENCES

[1] Kaminski, M.D., Nunez. L. 1999. *Journal of Magnetism and Magnetic Materials*.194.31-36.

[2] Shaibu, B.S., Reddy, M.L.P., Bhattacharyya, A., Manchanda, V.K. 2006. *Journal of Magnetism and Magnetic Materials* . 301. 312–318.

[3] Leslie-Pelecky, D.L., Rieke, R.D. 1996. *J. Chem. Mater.* 8 . 1770–1783

[4] Devi, M., Fingerman, M. *B.* 1995. *Environ.Contam.Tox*. 55.746–750.

[5] Zhang, F.S., Nriagu, J.O., Itoh. H. 2005. *J.Water Res.* 39 . 389–395.

[6] Uzun, L., Kara, A., Tüzmen, N., Karabakan, A., Besirli, N., Denizli, A. 2006. *J. Appl. Polym. Sci.* 102.4276–4283.

[7] Chen, C.Y., Lin, M.S., Hsu, K.R. 2008. *J. Hazard. Mater.* 152 . 986–993.

[8] Rivas, B.L., Pooley, S.A., Maturana, H.A., Villegas, S. 2001. *J.Macromol. Chem. Phys.* 202 . 443–447.

[9] Zhou, D., Zhang, L., Zhou, J., Guo. S. 2004 . *J. Water. Res.* 38 .2643–2650.

[10] Oliveira, L.C.A., Rios, R.V.R.A.,.Fabris, J.D., Sapag, K.; Garg, V.K., Lago. R.M. 2003. *J Appl. Clay Sci.* 22.169–177.

[11] Fan, F.L., Qin, Z.; Bai, J., Rong, W.D., Fan, F.Y.,Tian, W., Wu, X.L.,Wang, Y., Zhao, L. 2012. *J. Enviro. Radio.* 106. 40.

[12] Nunez, L., Kaminski, M., Bradley, C., Buchholz, B.A., Landsberger, S.; B.Aase, S., Tuazon, H.E., 1995. *Argonne National Laboratory, Chemical Technology Division.* ANL-95/1.

[13] Nunez, L., Kaminski, M.D. 1999. *Journal of Magnetism and Magnetic Materials*. 194. 102-107.

[14] Buchholz, B.A.; Tuaazon, H.E. , Kaminski, M.D., Aase, S.B.; Nunez, L., Vandegrift. G.F. 1997. *J. Sep and Pur. Tech.* 11 . 21 l-219.

[15] Nunez, L., Kaminski, M., Bradley, C., Buchholz, B.A., Landsberger, S., Aase, S.B.,Tuazon, H.E., Vandergrift, G.F., 1995.*Argonne National Laboratory, Chemical Technology Division.* ANL-95/26.

[16] Nunez, L.; Buchholz, B.A.; Ziemer, M.; DyrKacz, G.; Kaminski , M.; Vandergrift, G.F.; Atkins. K. 1994. *Argonne National Laboratory, Chemical Technology Division.,* ANL-94/47.

[17] Sadeghi, S., Azhdari, H.; Arabi, H.,Moghadam. A.Z. 2012. *J. hazardeous materials*. 2015.216. 208-216.

[18] Sadeghi, S., Aboobakri. E. 2012.*J. Microchem acta* . 178. 89-97.

[19] Leal, R., Yamaura. M. 2011.Journal of Nuclear Energy Science and Technology. 6. 1-7.

[20] Ngomsik, A., Bee, A., Draye, M.; Cote, G., Cabuil,V. 2005. *J. C. R. Chimie.* 8. 963–970.

[21] Teja, A. S., Koh, P.Y. 2008. *J. Progress in Crystal Growth and Characterization of Materials*. 1-24.

[22] Ambashtaa, R. D., Yusufb, S. M., Mukadamb, M. D., Singhb, S., Kishan, P.W., Bahadur. D. 2005. *Journal of Magnetism and Magnetic Materials.* 293. 8–14.

[23] Faraji, M.,Yamini, Y., Rezaee, M. 2010. *J. Talanta.* 81. 831–836.

[24] Klug, H.P., Alexander, L.E. 1962. *X-ray Diffraction Procedures for Polycrystalline and Amorphous Materials*, John Wiley & Sons, New York. p. 491.

[25] Meinrath, G. 1998. *Aquatic Chemistry of Uranium: A Review Focusing on Aspects of Environmental Chemistry. Frieberg on-line geoscience*. vol 1.

[26] Das, D., Sureshkumar, M.K., Koley, S., Mithal, N., Pillai, C.G.S. 2010. *J.chem.Thermodyn*. 41. 829-835.

[27] Humelnicu, D., Popovici, E., Mita, C. 2009. *J.Radioanal. Nucl. Chem.* 279.131-136.

[28] Han, R., Zou, W.Y., Wang, Zhu, L. 2007. *J. Environ. Radioact* . 93. 127-143.

[29] Yusan, S., Erenturk, S. . 2011.*J. Desalination.* 269. 58-66.

[30] Donat, R. 2009. *J. Chem*. *Thermodyn.* 41. 829-835.